



How Breathing and Cardiac functions interact with Cerebral arterio-venous blood flows: Origin of CSF oscillations

Pan LIU, Kimi Owashi, Heimiri Monnier, Cyrille Capel, Serge Metanbou, Olivier Balédent

► To cite this version:

Pan LIU, Kimi Owashi, Heimiri Monnier, Cyrille Capel, Serge Metanbou, et al.. How Breathing and Cardiac functions interact with Cerebral arterio-venous blood flows: Origin of CSF oscillations. ISMRM 2024, International Society for Magnetic Resonance in Medicine, May 2024, Singapoore, Singapore. <10.58530/2024/4923>. <hal-04627956>

HAL Id: hal-04627956

<https://hal.science/hal-04627956v1>

Submitted on 28 Jun 2024

HAL is a multi-disciplinary open access archive for the deposit and dissemination of scientific research documents, whether they are published or not. The documents may come from teaching and research institutions in France or abroad, or from public or private research centers.

L'archive ouverte pluridisciplinaire **HAL**, est destinée au dépôt et à la diffusion de documents scientifiques de niveau recherche, publiés ou non, émanant des établissements d'enseignement et de recherche français ou étrangers, des laboratoires publics ou privés.



HAL Authorization

How Breathing and Cardiac functions interact with Cerebral arterio-venous blood flows: Origin of CSF oscillations

Pan Liu^{1,2}, Kimi Owashi¹, Heimiri Monnier¹, Serge Metanbou³, Cyrille Capel^{1,4}, Olivier Balédent^{1,2}

¹ CHIMERE UR 7516, Jules Verne University of Picardy, Amiens, France

² Medical Image Processing Department, Amiens Picardy University Hospital, Amiens, France

³ Radiology Department, Amiens Picardy University Hospital, Amiens, France

⁴ Neurosurgery Department, Amiens Picardy University Hospital, Amiens, France

Synopsis

Motivation

The main drivers of CSF oscillations are currently controversial.

Goal

To investigate whether the breathing or cardiac regulated Cerebral blood flow are the major driver of CSF dynamics.

Approach

Investigate Cerebral blood and CSF flows through the intracranial compartment during free and deep breathing using real-time phase-contrast sequence. To quantify the neurofluids volume displacement along the cardiac cycle.

Results

Both cardiac and breathing cycles influenced neurofluids volume displacements. CSF dynamics is significantly correlated with intracranial blood volume change. CSF dynamic acts as a compensatory mechanism of intracranial blood volume dynamics.

Impact

This study confirms that intracranial blood volume change due to cardiac and breathing activities are the main drivers of CSF dynamic. This study provides valuable insights for understanding CSF circulation's complex mechanism and investigating idiopathic cerebral diseases.

Introduction

Although changes in cerebral blood volume (CBV) were initially recognized as the major driver of cerebrospinal fluid (CSF) oscillations^{1,2}, recent advances in real-time phase-contrast MRI (RT-PC) have revealed the influence of breathing on CSF dynamics^{3,4,5}. New mechanistic hypotheses challenging the established Monro-Kellie doctrine have emerged, such as CSF flow is driven by the thoracic and lumbar spina⁶.

Therefore, quantifying both CBV and CSF displacement volume (CSFV) under the influence of breathing will provide a better understanding of CSF dynamics. The aim of this study was to measure the CBV and CSFV during free- and deep-breathing patterns using RT-PC to investigate whether the breathing-modulated CBV fluctuations are the main driving force of CSF oscillations.

Methods

– Image acquisition

12 healthy volunteers (age: 20~34) were examined using a clinical 3T scanner and a 32-channel head coil. A finger plethysmograph and a respiratory chest were used to record pulse and breathing signals synchronously during acquisition. Each imaging level was acquired twice: once during free-breathing and once during deep-breathing.

For quantification purposes, the intracranial level was selected for CBV measurements, while the extracranial level, C2-C3, was used for CSF measurements. The RT-PC used in this study was a multi-shot, gradient-recalled echo-planar imaging sequence with parallel acquisition technology. Parameters were: SENSE=2.5, EPI-factor=7, FOV=140*140mm², matrix acquisition=70*70mm². Other parameters are shown in Fig.1-A.

– Extraction of CBV and CSFV

All image and signal processing were performed using in-house software – Flow 2.0^{7,8}.

Arterial inflow, venous outflow, and CSF oscillations were extracted through post-processing steps, including image segmentation, background field correction, and de-aliasing⁹.

Venous outflow was adjusted to account for unconsidered peripheral venous drainage and maintain a mean venous flow equal to the mean arterial flow. Subsequently, cerebral blood flow (CBF) was calculated as the sum of the arterial inflow and venous outflow (Fig.1-B).

The CBF and CSF flow signals were then integrated over time to obtain CBV and CSFV signals, respectively. Finally, to preserve the breathing and cardiac frequency components, both volume signals underwent baseline drift correction and high-pass filtering (>0.1 Hz) (Fig.1-C).

– Reconstruction of Cardiac- and Breath-Volume Displacement Signals

Pulse and breathing signal peaks were identified to segment the volume curves according to the multiple cardiac and respiratory cycles (Fig.2-A&A'). This resulted in reconstructed cardiac-CBV/CSFV and Breath-CBV/CSFV curves, capturing the mean volumetric changes across these physiological cycles (Fig.2-B).

The analysis of the reconstructed volume curves aimed to quantify the breathing effects and to investigate the CBV-CSFV correlation.

Results

Fig.3 demonstrates that during deep-breathing, compared to free-breathing, inflow decreases by 29%. Cardiac-CBV and Cardiac-CSFV amplitudes decrease by 37% and 23%, respectively, partly due to a 15% shorter cardiac cycle. Conversely, Breath-CBV and Breath-CSFV amplitudes increase by 207% and 326%.

Fig.4 illustrates that in both breathing states, a significant correlation was presented between the amplitudes of Cardiac-CBV and Cardiac-CSFV, as well as between the amplitudes of Breath-CBV and Breath-CSFV. No significant amplitude differences were observed between Cardiac/Breath-CBV and Cardiac/Breath-CSFV during deep-breathing. Moreover, Cardiac-CBV/CSFV amplitudes are cardiac period dependent, whereas Breath-CBV/CSFV amplitudes correlate with the breathing period only during deep-breathing.

During free-breathing, CSF flows consistently toward the intracranial compartment during inspiration. However, deep-breathing induces significant phase shifts in three cases, marked in red in Fig.5.

Discussion

Free-breathing can affect CBF and CSF flow¹⁰; therefore, CBV changes must be considered in CSF dynamics studies¹¹. This study demonstrates a strong correlation between CBV and CSFV displacements due to cardiac and breathing activities.

Using pulse and breathing signals for segmentation and reconstruction of Cardiac-CBV/CSFV and Breath-CBV/CSFV partially overcomes the challenges of simultaneous CBF and CSF measurements. This study demonstrated a clear symmetry between CBV and CSFV. Moreover, this approach facilitates the observation of the volume displacement direction during the different respiratory phases.

The ability of CSF to regulate CBV changes was more pronounced during deep-breathing (Fig.4). This interesting phenomenon is possibly related to alterations in intracranial compliance; however, further investigation is worthwhile.

Although ultra-low frequency components (<0.1 Hz) of CBV and CSFV were observed, they were not analyzed in this study due to frequency resolution limitations. Future studies could further investigate this phenomenon.

Conclusion

This study confirms that changes in CBV resulting from cardiac and breathing activities are the main drivers of CSF dynamics, the free physiological breathing activity makes a minor contribution to CSF dynamics. This study provides valuable insights into the mechanism of CSF circulation and its potential clinical diagnostic applications in certain diseases.

Figures (5/5)

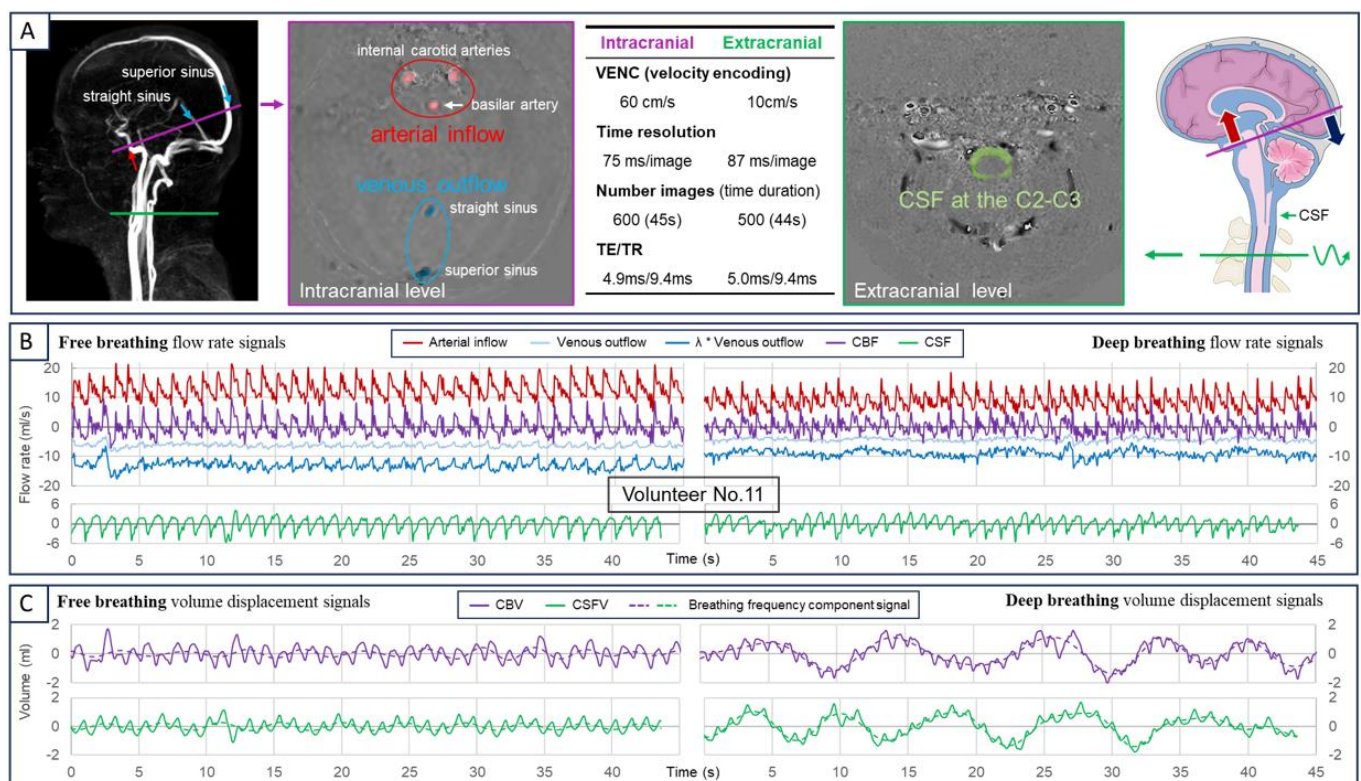


Figure 1: A) Imaging levels and RT-PC parameters. The intracranial section comprises three arteries and two sinuses. B) Flow curves obtained via post-processing software. CBF is the sum of inflow and $\lambda \cdot$ outflow, where λ represents the ratio between mean inflow and outflow values. C) After integrating the CBF and CSF curves, baseline drift is removed, and ultra-low frequencies below 0.1 Hz are filtered, resulting in the final CBV and CSFV curves.

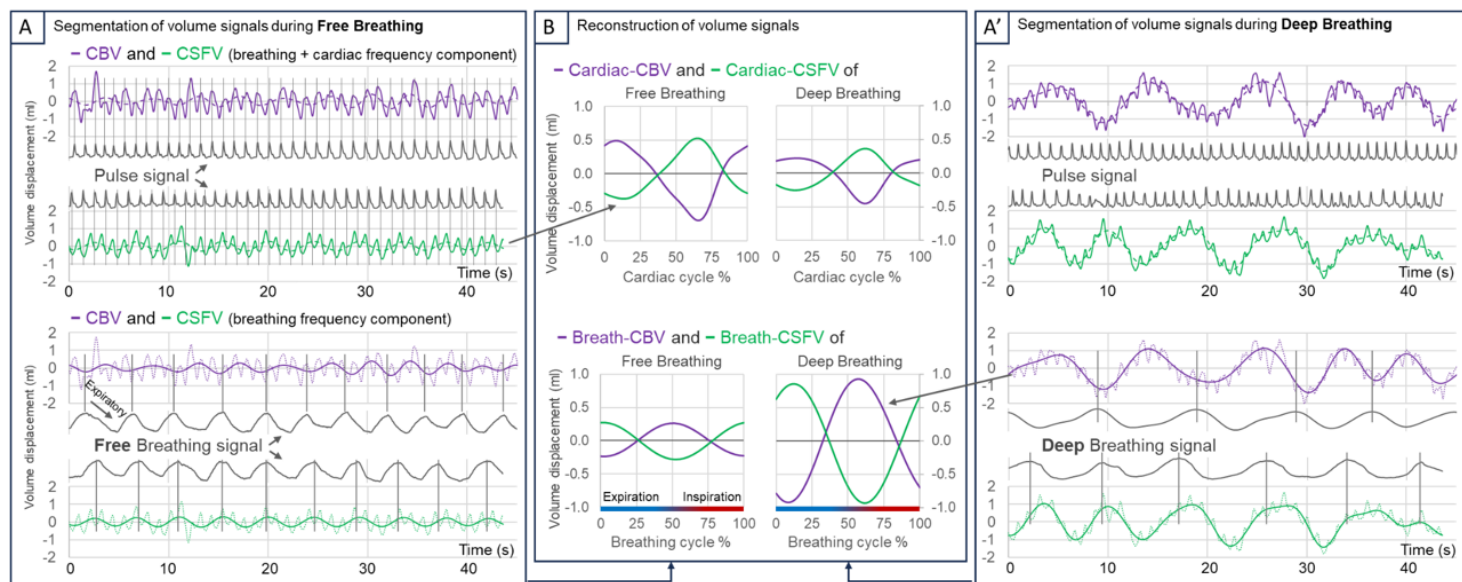


Figure 2: The CBV and CSFV under free breathing (A) and deep breathing (A') were segmented into multiple independent volume curves using pulse and breathing signals. B) Reconstruction of the independent cardiac cycle volume curves as Cardiac-CBV and Cardiac-CSF. Reconstruction of the independent breathing cycle volume curves as Breath-CBV and Breath-CSFV.

	Mean value	Mean value	λ	Cardiac-CBV	Cardiac-CSFV	Cardiac Period	Breath-CBV	Breath-CSFV	Breathing period
	Inflow (ml/s)	Outflow (ml/s)		Amplitude (ml)	Amplitude (ml)	(s)	Amplitude (ml)	Amplitude (ml)	(s)
Free Breathing	12.5 ± 1.8	7.9 ± 1.6	1.6 ± 0.2	0.74 ± 0.2	0.58 ± 0.2	0.90 ± 0.2	0.47 ± 0.2	0.33 ± 0.2	3.7 ± 0.4
Deep Breathing	8.8 ± 1.6	5.3 ± 0.8	1.7 ± 0.3	0.47 ± 0.1	0.45 ± 0.1	0.77 ± 0.2	1.44 ± 0.9	1.40 ± 0.7	6.2 ± 2.2
(Deep vs. Free)									
Difference %	-29%	-33%	4%	-37%	-23%	-15%	207%	326%	67%
p value (paired t-test)	**	**		**	**	**	**	**	**
p value (pearson test)		**	**	*	**	**			

Figure 3: Results of each parameter under free breathing and deep breathing. The data of each group were detected by the Shapiro-Wilk test normal distribution. Differences in mean values and correlations of parameters under both breathing modes were analyzed using t-test and Pearson's test. Statistical significance was denoted by * for p-value < 0.05 and ** for p-value < 0.01.

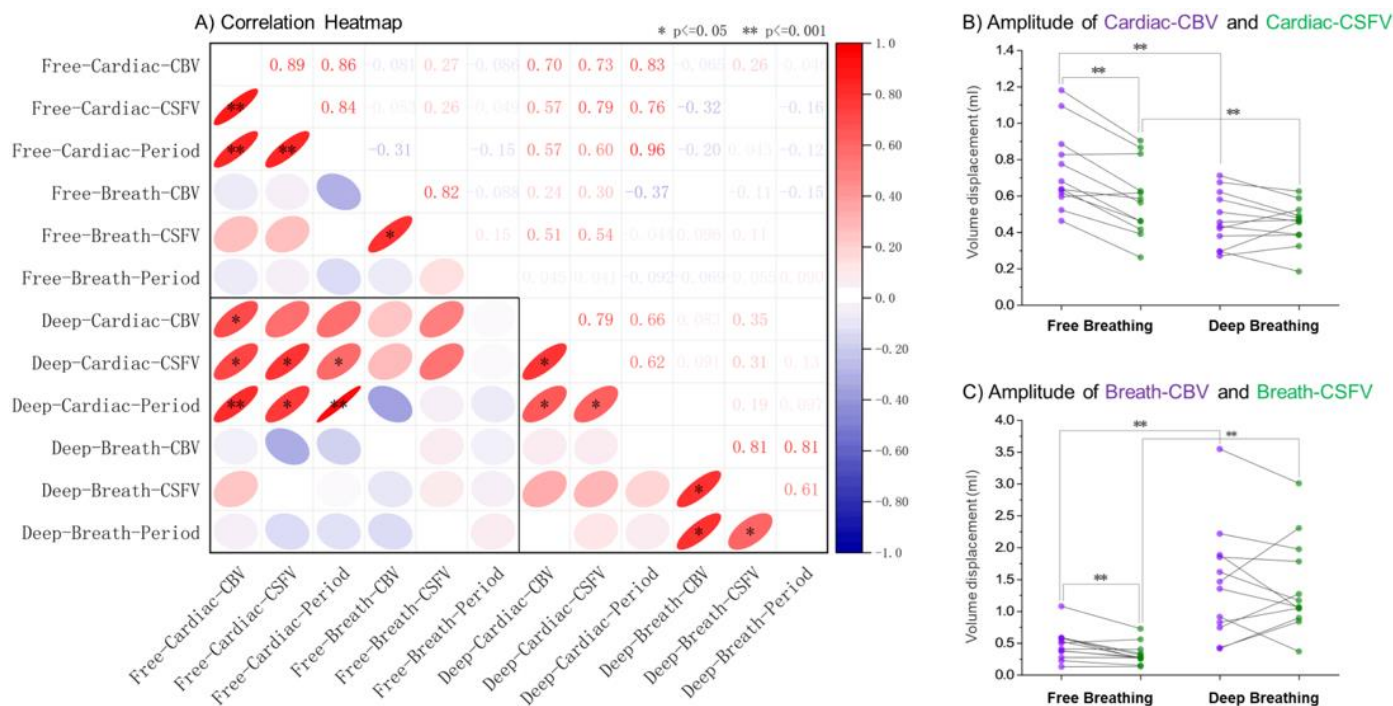


Figure 4: A) Correlation heatmap (Pearson's test) of each parameter during free and deep breathing. Free-Cardiac-CBV indicates the amplitude of the Cardiac-CBV curve under free breathing, Deep-Breath-CSFV indicates the amplitude of the Breath-CSFV curve under deep breathing. B) The distribution of amplitudes for Cardiac-CBV and Cardiac-CSFV under the two breathing patterns. C) The distribution of amplitudes of Breath-CBV and Breath-CSFV under the two breathing patterns.

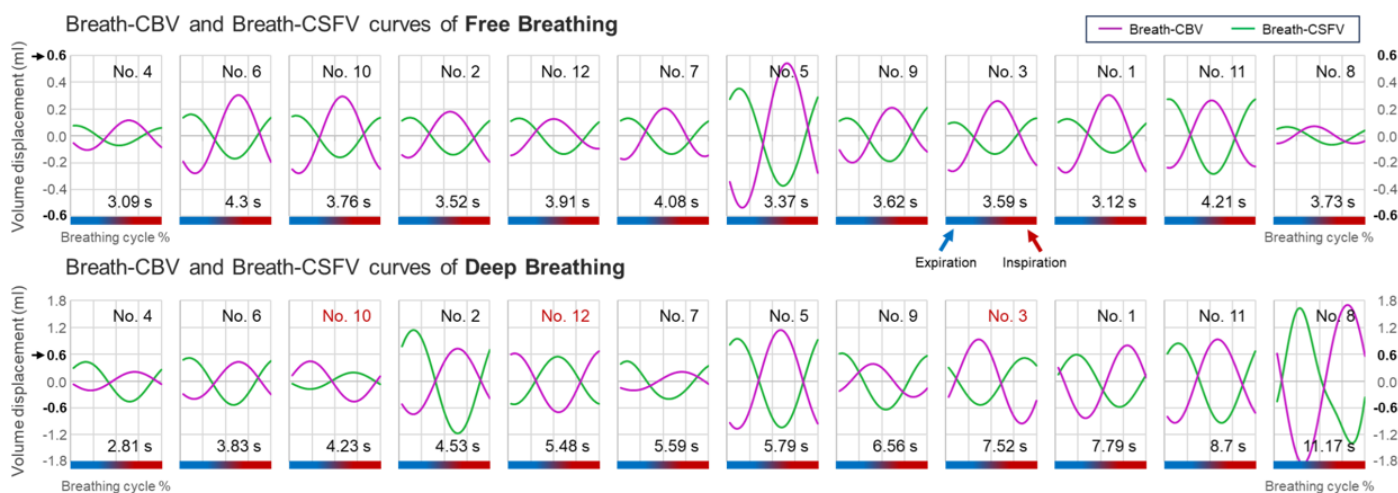


Figure 5: Breath-CBV (purple) and Breath-CSFV (green) curves for all participants during free breathing (top) and deep breathing (bottom) patterns. The curves are arranged in ascending order of deep breathing period. The y-axis represents the volume displacement (-0.6ml~0.6ml for free breathing and -1.8ml~1.8ml for deep breathing), and the x-axis denotes the percentage of the breathing period from expiration (blue) to inspiration (red). The breathing period is labeled in each plot.

References

1. Balédent O, Idy-peretti I. Cerebrospinal fluid dynamics and relation with blood flow: a magnetic resonance study with semiautomated cerebrospinal fluid segmentation. *Investigative radiology*. 2001 Jul 1;36(7):368-77.
2. Alperin N, Lee SH, Loth F, Raksin P, Lichtor T. MR-Intracranial Pressure (ICP): A method for noninvasive measurement of intracranial pressure and elastance. Baboon and Human Study. *Radiology*. 2000;217(3):877-85. <https://doi.org/10.1148/radiology.217.3.r00dc42877>.
3. Balédent O, Liu P, Lokossou A, Fall S, Metanbou S, Makki M. Real-time phase contrast magnetic resonance imaging for assessment of cerebral hemodynamics during breathing. In ISMRM 2019-International Society for Magnetic Resonance in Medicine 2019 May 11. <https://hal.archives-ouvertes.fr/hal-03736882>.
4. Yildiz S, Thyagaraj S, Jin N, Zhong X, Heidari Pahlavian S, Martin BA, Loth F, Oshinski J, Sabra KG. Quantifying the influence of respiration and cardiac pulsations on cerebrospinal fluid dynamics using real-time phase-contrast MRI. *Journal of Magnetic Resonance Imaging*. 2017 Aug;46(2):431-9. <https://doi.org/10.1002/jmri.25591>.
5. Gutiérrez-Montes, C., W. Coenen, M. Vidorreta, S. Sincomb, C. Martínez-Bazán, A. L. Sánchez, and V. Haughton. "Effect of Normal Breathing on the Movement of CSF in the Spinal Subarachnoid Space." *American Journal of Neuroradiology* 43, no. 9 (September 1, 2022): 1369–74. <https://doi.org/10.3174/ajnr.A7603>.
6. Lloyd, Robert A., Jane E. Butler, Simon C. Gandevia, Iain K. Ball, Barbara Toson, Marcus A. Stoodley, and Lynne E. Bilston. "Respiratory Cerebrospinal Fluid Flow Is Driven by the Thoracic and Lumbar Spinal Pressures." *The Journal of Physiology* 598, no. 24 (2020): 5789–5805. <https://doi.org/10.1113/JP279458>.
7. Liu P, Lokossou A, Fall S, Makki M and Bamendent O, 2019. Post Processing Software for Echo Planar Imaging Phase Contrast Sequence. ISMRM 27th, (4823). <https://archive.ismrm.org/2019/4823.html>
8. Liu P, Fall S, Balédent O. Flow 2.0-a flexible, scalable, cross-platform post-processing software for realtime phase contrast sequences. In ISMRM 2022-International Society for Magnetic Resonance in Medicine 2022 May 7. <https://archive.ismrm.org/2022/2772.html>
9. Liu P, Fall S, Balédent O. Use of real-time phase-contrast MRI to quantify the effect of spontaneous breathing on the cerebral arteries. *NeuroImage*. 2022 Jun 7;119361. <https://doi.org/10.1016/j.neuroimage.2022.119361>.
10. Liu P, Monnier H, Owashi K, Constant JM, Capel C, Balédent O. "The Effects of Free Breathing on Cerebral Venous Flow: a real-time phase contrast MRI study in healthy adults". *The Journal of Neuroscience* 44, no. 3 (January 17, 2024): e0965232023. <https://doi.org/10.1523/JNEUROSCI.0965-23.2023>.
11. Burman, R., & Alperin, N. (2023). CSF-to-blood toxins clearance is modulated by breathing through cranio–spinal CSF oscillation. *Journal of sleep research*, e14029. <https://doi.org/10.1111/jsr.14029>.

Acknowledgements

This research was supported by EquipEX FIGURES (Facing Faces Institute Guilding Research), Hanuman ANR-18-CE45-0014 and Region Haut de France.

Thanks to the staff members at the Facing Faces Institute (Amiens, France) for technical assistance.

Thanks to David Chechin from Phillips industry for his scientific support.